Virology 391 (2009) 99–106

Contents lists available at ScienceDirect

Virology

journal homepage: www.elsevier.com/locate/yviro

Characterization of the guinea pig cytomegalovirus genome locus that encodes homologs of human cytomegalovirus major immediate-early genes, UL128, and UL130

Souichi Yamada [a], Naoki Nozawa [a], Harutaka Katano [b], Yoshiko Fukui [a], Mihoko Tsuda [a], Yoshihiro Tsutsui [c,1], Ichiro Kurane [a], Naoki Inoue [a,*]

[a] Department of Virology I, National Institute of Infectious Diseases, 1-23-1 Toyama, Shinjuku-ku, Tokyo 162-8640, Japan
[b] Department of Pathology, National Institute of Infectious Diseases, Tokyo, Japan
[c] Department of Pathology II, Hamamatsu Medical University, Shizuoka, Japan

ARTICLE INFO

Article history:
Received 30 March 2009
Returned to author for revision 21 May 2009
Accepted 22 May 2009
Available online 26 June 2009

Keywords:
Genome sequence
RACE
Virion
Glycoprotein
Immediate-early protein
UL128
UL130
Cytomegalovirus
Guinea pig

ABSTRACT

We reported previously that the guinea pig cytomegalovirus (CMV) stock purchased from the American Type Culture Collection contained two types of strains, one containing and the other lacking a 1.6 kb locus, and that the 1.6 kb locus was required for efficient viral growth in animals but not in cell culture. In this study, we characterized the genetic contents of the locus, and found that i) the 1.6 kb locus encodes homologs of human CMV UL128 and UL130, GP129 and GP131, respectively, ii) these genes are expressed with late gene kinetics, iii) GP131 protein (pGP131) localized to cell surface only in the presence of glycoproteins H and L, and iv) pGP131 is a virion component. Therefore, it is plausible that pGP131 forms a complex with glycoproteins H and L and becomes a virion component as does UL130 protein (pUL130). Since pUL130 is one of the glycoproteins essential for infection of endothelial and epithelial cells in human and primates, functional and immunological analyses of this GPCMV homolog of pUL130 may help to illuminate the in vivo role of pUL130.

Introduction

Human cytomegalovirus (HCMV) is the most common cause of congenital virus infection. Congenital infection occurs in 0.2–1% of all births, and causes birth defects and developmental abnormalities, including sensorineural hearing loss (SNHL) and developmental delay (Koyano et al., 2009; Ogawa et al., 2007; Pass, 2001). Animal models are generally valuable for understanding pathogenesis as well as developing therapeutics for infectious diseases. In contrast to murine CMV (MCMV) and rat CMV (RCMV), guinea pig CMV (GPCMV) crosses the placenta and causes infection in utero. This makes GPCMV animal models useful for studies on the mechanisms of transplacental transmission of CMV as well as for evaluation of vaccines, antiviral drugs, and passive antibody to prevent congenital CMV diseases (reviewed in Schleiss, 2006; Kern, 2006). We demonstrated congenital CMV-associated labyrinthitis in a guinea pig model in which vertical infection by GPCMV occurred through the placenta (Katano et al., 2007). During the characterization of GPCMV genome structure, we noticed that the GPCMV stock purchased from the American Type Culture Collection (ATCC) is a mixture of two strains, one containing and the other lacking a 1.6 kb locus, designated as GPCMV/full and GPCMV/del, respectively (Nozawa et al., 2008). Importantly, the 1.6 kb locus was required for efficient viral growth in animals but not in cell culture. Based on the location of the locus and a weak similarity of one of the ORFs in the locus with HCMV UL130, we hypothesized that the locus may correspond to the HCMV locus encoding UL128–UL131A.

Endothelial cells and leukocytes may play an important role in dissemination of HCMV in vivo, and viral replication in such cells is likely to contribute to HCMV pathogenesis (Gerna et al., 2004; Grundy et al., 1998). It is well known that passages of HCMV isolates in fibroblast cells results in the loss of growth ability in epithelial and endothelial cells. Several studies demonstrated that the growth defect was associated with genetic alterations, including ORF-disrupting mutations and deletions, in the UL128–150 region (Dolan et al., 2004; Cha et al., 1996; Murphy et al., 2003). It has been reported that UL128, UL130 and UL131A in the locus are essential for infection of endothelial and epithelial cells, and also for viral transmission to leukocytes (Adler et al., 2006; Wang and Shenk, 2005a, 2005b; Ryckman et al., 2006; Hahn et al., 2004). These genes encode glycoproteins that form a complex with glycoproteins H (gH) and L

* Corresponding author. Fax: +81 3 5285 1180.
E-mail address: ninoue@nih.go.jp (N. Inoue).
[1] Present affiliation: Faculty of Health Sciences, Hamamatsu University.

0042-6822/$ – see front matter © 2009 Elsevier Inc. All rights reserved.
doi:10.1016/j.virol.2009.05.034

Table 1
Differences in the GPCMV sequences.

This study		Schleiss et al. (2008)		Effects
Position	Sequence	Position	Sequence	
1		188,197		
143	A	188,339	AA	IE2 exon 5 frame shift
255	C	188,452	T	IE2 aa substitution
447	A	188,644	T	IE2 aa substitution
1038	G	189,235	GG	IE2 exon 5 frame shift
2365	G	190,563	T	IE1 aa substitution
2575	T	190,774	G	IE1 aa substitution
2728	G	190,927	T	IE1 aa substitution
2737	G	190,936	GG	IE1 exon 5 frame shift
2879	G	191,079	A	Silent
2931	G	191,131	A	IE1 aa substitution
2966	A	191,176	AT	IE1 exon 5 frame shift
2968	TG	191,078	AT	IE1 aa substitution
3758	T	191,958	G	Silent (intron)
8701	T	196,901	TGAATAAAACT	GP129 exon 3 frame shift
8908	TTGTT	197,118	T	GP129 exon 3 frame shift
9134	T[a]	197,340	G	Silent (intron)
12,920		201,126		

[a] G in a part of ATCC-derived virus stocks.

(gL) (Ryckman et al., 2008b) and localize in virion particles (Wang and Shenk, 2005b).

In this study, we characterized the genetic contents in and in the vicinity of the 1.6 kb locus, and found that GPCMV encodes biologically similar orthologs of HCMV UL128 and UL130.

Results

Comparison of the sequences containing the major immediate-early genes and the 1.6 kb locus between GPCMV passaged in tissue culture and that grown in animals

The complete genome sequence of GPCMV that was derived from the ATCC stock and cultured in vitro was recently reported (Schleiss et al., 2008). However, i) no HCMV UL123 (IE1) homolog was identified in their sequence, ii) the sequence of the open reading frame (ORF) annotated for UL122 (IE2 exon 5) is different from that previously reported by us (Nozawa et al., 2008), and iii) it is well known that human and rhesus cytomegaloviruses cultured in vitro accumulate genetic alterations in the UL128–UL131A locus. Therefore, from a collection of four GPCMV strains that differ in their in vivo and in vitro passage histories, we determined the DNA sequences of a 13 kb genomic segment that spans the major immediate-early gene locus and the locus that potentially corresponds to UL128–UL131A. Each of the four virus strains studied grew efficiently in animals. They include: i) a virus stock passaged in vitro five times from the original ATCC stock in GPL cells (TC-P5), ii) a supernatant of sonicated salivary glands from a guinea pig that was sacrificed 21 days after the inoculation with GPCMV (SG-P0), iii) a virus stock passaged 5 times in vitro after infection of GPL cells with the SG-P0 stock (SG-P5), and iv) one GPCMV/full virus stock that was passaged 5 times in vitro after virus cloning from a stock obtained from ATCC (CD-P5). The sequence of SG-P0 and the published sequence had significant differences as

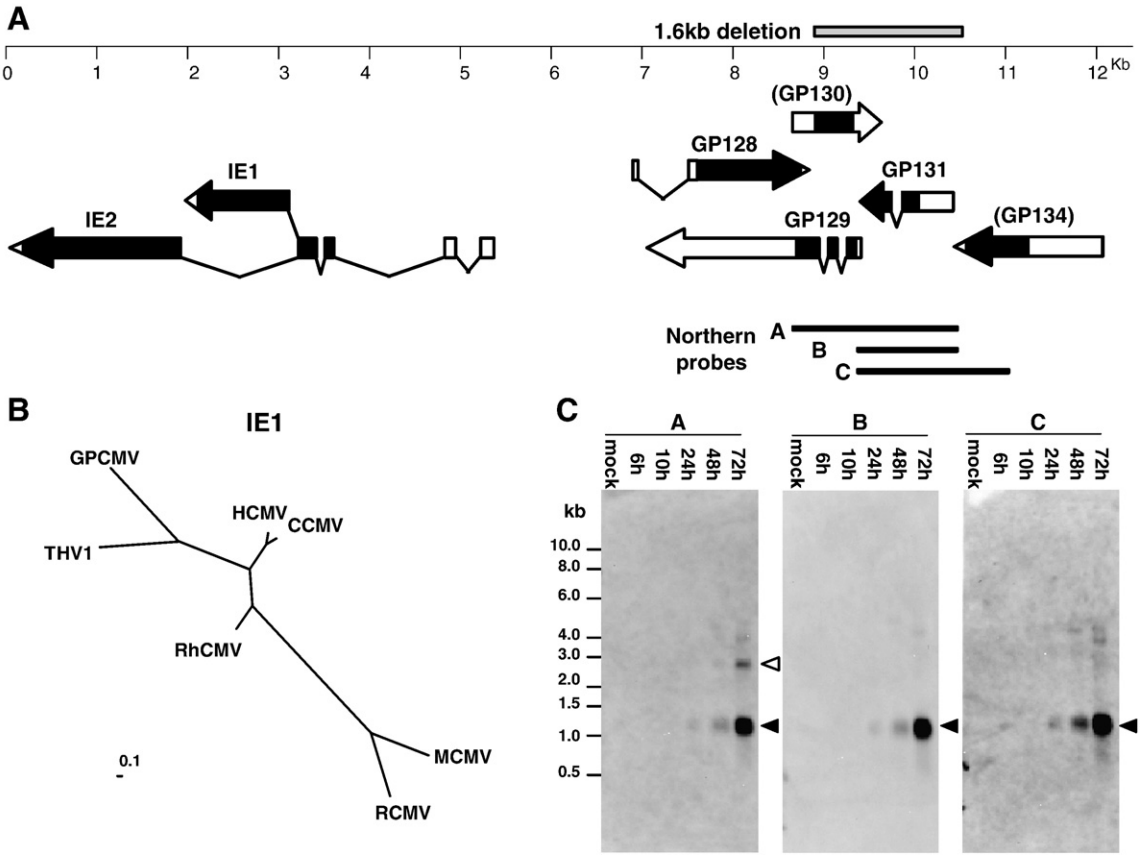

Fig. 1. (A) Transcription units identified by RACE in the 13 kb region of GPCMV. The 1.6 kb locus essential for efficient growth in vivo is shown as a hatched box on top of the scale. Non-coding and coding regions are indicated as open and closed boxes/arrows, respectively. ORFs for which transcripts were not detectable in the Northern blotting (panel C) are shown in parentheses. Probes A to C were used for the Northern blotting analysis. (B) Phylogenic dendrogram of IE1 exon 5, including MCMV, RCMV, chimpanzee CMV (CCMV), HCMV, rhesus CMV (RhCMV), simian CMV (SCMV), and tupaia herpesvirus 1 (THV1). GenBank accession numbers of these sequences were U68299, AF232689, AF480884, AY446894, AY186194, U38308, and AF281817, respectively. (C) Northern blotting analysis of the 1.6 kb region. RNA samples prepared from GPL cells that were infected with GPCMV and harvested at the indicated times after inoculation were analyzed. Open and closed arrowheads indicate the GP129 and GP131 transcripts. As size standards, 0.5–10 kb RNA ladder (Invitrogen) was used.

Table 2
Transcripts and ORFs identified by RACE analysis.

Gene name		Transcript		ORF	
		Start	End	Start	Stop
IE1/2	TATA[a]	5324			
	Exon 1	5295	5120		
	Exon 2	4942	4799		
	Exon 3	3631	3518	3630	
	Exon 4	3428	3196		
IE1 (*GP123*[b])	Exon 5	3108	1860		2030
	polyA[a]	1882			
IE2 (*GP122*)	Exon 5	1818	8		134
	polyA[a]	34			
GP128[b]	TATA[a]	6845			
	Exon 1	6875	6948		
	Exon 2	7516	8784	7638	8693
	polyA[a]	8764			
GP129	TATA[a]	NA			
	Exon 1	9418	9210	9364	
	Exon 2	9131	9006		
	Exon 3	8928	7056		8670
	polyA[a]	7071			
GP130	TATA[a]	8593			
	Gene	8623	9584	8893	9285
	polyA[a]	9552			
GP131	TATA[a]	10,457			
	Exon 1	10,424	9786	10,027	
	Exon 2	9705	9364		9369
	polyA[a]	9430			
GP134	TATA[a]	12,080			
	Gene	12,048	10,417	11,187	10,504
	polyA[a]	10,445			
1.6 kb deletion		8847	10,495		

[a] First base of the TATA box and polyA signal is indicated.
[b] Designated based on the homology with M128 and R128, although it was described as *GP123* recently (Schleiss et al., 2008).

summarized in Table 1. TC-P5 was a mixture of viruses with and without the 1.6 kb deletion as we reported previously and it had a sequence of both G and T at position 9134. However, the remaining part was identical with SG-P0. Importantly, SG-P5 and CD-P5 were identical with SG-P0. Therefore, the differences with the published sequence might be due to differences in in vitro passage history or to sequencing a particular virus cloned as a BAC.

Gene organization

We reported the *IE2* gene structure and demonstrated the expression of the IE2 transcript previously (Nozawa et al., 2008). In this study we extended the analysis of GPCMV genetic content and gene expression to the 13 kb region described above. For this purpose, we performed 5′ and 3′ RACE experiments using various primers. We identified five transcription units in addition to IE1 and IE2 transcription units (Fig. 1A). The details of the intron/exon structures and potential TATA-boxes and poly(A) signals are summarized in Table 2. The predicted differences in protein coding potential between the published GPCMV sequence and the sequences we determined for the SG-P0, SG-P5, and CD-P5 viruses are summarized in Table 1. Notably, the two sequences lead to significant changes in the predicted amino acid sequences. For example, the frame shift alterations at positions 188,339 and 189,235 in the published sequence disturb the coding contents of IE2 exon 5 (GP122). Similarly, the insertions at 190,936 and 191,176 made identification of GP123, a homolog of IE1 (UL123), impossible in the published sequence. In our sequences, GP123 was recognizable as IE1 exon 5 with unambiguous homology with MCMV M123, RCMV R123-EX4, RhCMV Rh156, THV1 t123 and HCMV UL123. Their amino acid (a.a.) sequence similarities are 56, 56, 57, 57 and 59%, respectively. Phylogenetic analysis of IE1 places GPCMV at similar distances between rodent and primate CMVs, as observed previously for IE2 (Fig. 1B). Based on the designations for orthologous genes in other CMVs, we designate IE1 exon 5 as GP123 and a homolog of MCMV M128 as GP128. Although these designations differ from those used in the report of the complete GPCMV genome sequence (Schleiss et al., 2008), the sequences of M128 homolog in both studies are exactly same.

Expression of GP129 and GP131 at the RNA level in vitro and in vivo

To exclude the possibility that RACE reactions amplified some artifactual products, expression of the transcription units for GP129, GP130, GP131 and GP134 was analyzed by Northern blotting. Probe A, which can theoretically detect all four of these transcripts, detected at least two transcripts of 2.8 kb (open arrowhead) and 1.2 kb (closed arrowhead) (Fig. 1C). Based on the lengths of the transcripts and additional information obtained from Probes B and C, the 2.8 kb and 1.2 kb transcripts are likely to be the transcripts for GP129 and GP131, respectively. Both transcripts were detectable from 24 h post infection. The transcripts were not detected after treatment of the infected cells with phosphonoacetic acid (PAA) (data not shown), suggesting that both *GP129* and *GP131* are late genes. The transcripts corresponding to GP130 and GP134 were not detectable in the blots.

To confirm the expression of GP129 and GP131 during the lytic growth phase of GPCMV infection, quantitative RT-PCR assays for detection of their transcripts were performed using probes S7 and S9 that targeted the splicing junctions (Supplementary table 1, Fig. 2A).

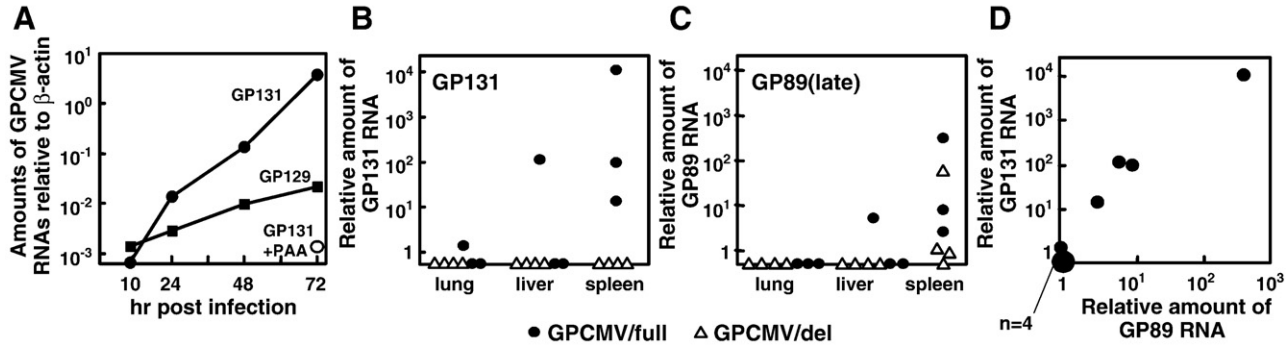

Fig. 2. Detection and quantification of GP129 and GP131 transcripts by quantitative RT-PCR assays. (A) RNA samples prepared from GPL cells that were infected with GPCMV and harvested at the indicated times after infection were used for the assays. S7, S9, and S10 (Supplementary table 1) were used as a set of primers/probe for the GP131, GP129 and β-actin transcripts, respectively. The amounts of the GP131 and GP129 transcripts relative to that of the β-actin transcripts were calculated based on differences in the threshold PCR cycle numbers. (B–D) RNA samples prepared from liver, lung, and spleen of guinea pigs infected with GPCMV/full (closed circles) and with GPCMV/del (open triangles). Relative amounts of the GP131 and GP89 transcripts were calculated based on threshold PCR cycle numbers, and normalized with weights of organs used for RNA preparation. Detection limit of the transcripts per mg of the organs in the assay was defined as 1.

In GPL cells, GP131 transcript levels increased significantly from 24 h post infection, while the GP129 transcripts accumulated gradually. The abundance of GP131 transcripts was >100-fold greater than for GP129 at 3 days post infection.

GP131 transcripts were expressed also in the livers and spleens of guinea pigs infected with GPCMV/full (Fig. 2B). Transcripts of the *GP89* gene encoding a late gene product, terminase, were detected in the animals infected both with GPCMV/full and with GPCMV/del (Fig. 2C). The amounts of the GP131 and GP89 transcripts in the GPCMV/full-infected animals showed a correlation (Fig. 2D).

Relationships among amino acid sequences of GP129 and GP131 with HCMV UL128 and UL130

The a.a. sequence of GP129 has 33% identity and 48% similarity with HCMV UL128 (Fig. 3). Very recently, a core region of HCMV pUL128 crucial for endothelial cell tropism has been mapped to a.a. positions 72 to 106 by charge cluster-to-alanine mutagenesis (Schuessler et al., 2008). The core region corresponds to the sequences that are highly homologous to other UL128 homologs, including GPCMV GP129. Interestingly, the second splicing junction

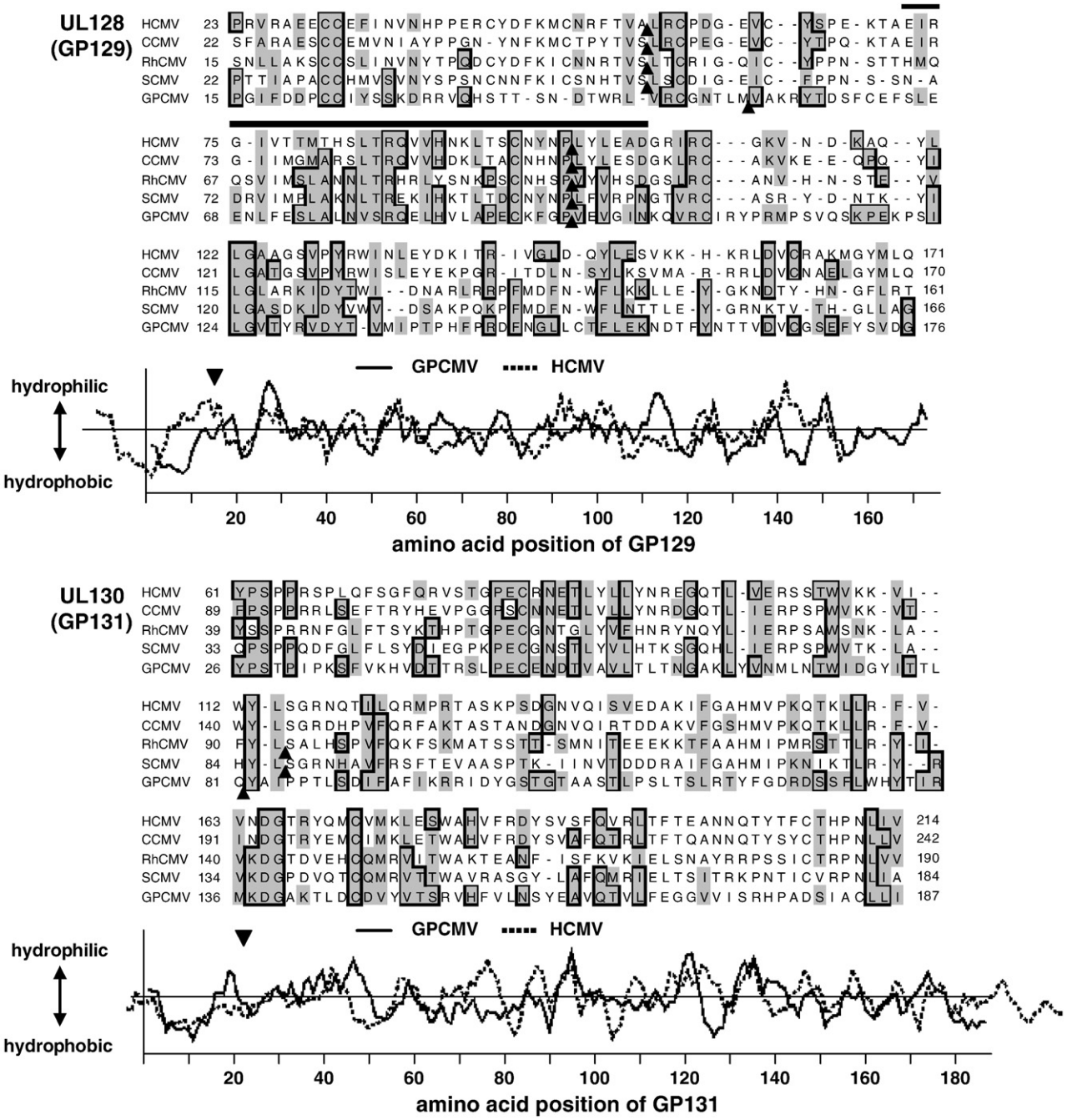

Fig. 3. Amino acid sequence homology of GP129 and GP131 with UL128 and UL130 homologs, respectively. Identical and homologous sequences to GPCMV were boxed and highlighted in gray, respectively. GenBank accession numbers of sequences used for comparison of UL128 and UL130 homologs are as follows: CCMV AF480884, RhCMV (strain 22659) EU130540, SCMV U38308, and HCMV (Merlin) AY446894. UL128 sequences of CCMV, SCMV and HCMV were corrected to the expected wild-type sequences based on the previous report (Akter et al., 2003). The core region of HCMV UL128 crucial for endothelial cell tropism (Schuessler et al., 2008) is shown with a closed bar on top of sequences. Arrowheads indicate the splice junctions in each ORF. Hydrophilicity/hydrophobicity plots of the GP129 and GP131 a.a. sequences generated by the software (GENETYX) based on the method of Hopp and Woods (1981). Areas above and below indicate hydrophilic and hydrophobic domains, respectively. Arrowheads indicate the predicted signal peptide cleavage sites of HCMV and GPCMV, and two plots were matched at the sites. The horizontal scale indicates the a.a. sequence positions of the GPCMV proteins.

located in the core region was well conserved among the UL128 homologs. The a.a. sequence of the GP131 ORF has 19% identity and 36% similarity with HCMV UL130. A potential N-glycosylation site of GP131 was predicted at a.a. positions 51–54, around which the sequences were highly homologous to HCMV UL130 (NetNGlyc 1.0 Server, www.cbs.dtu.dk/services/NetNGlyc/). Both GP129 and GP131 a.a. sequences posses signal sequences, but not transmembrane domains.

No CMV homolog for GP130 and GP134 were identified in GenBank. There was no recognizable homolog of HCMV UL131A in the vicinity of the *GP129* and *GP131* genes.

Detection of pGP131

Because the GP131 transcript is more abundant than the GP129 transcripts, we focused on GP131 in the following analyses. Antibody against GP131 protein was prepared by immunization of a rabbit with a partially-purified GST-GP131 fusion protein. Anti-GP131 detected a fluorescent signal in the GPL cells infected with CD-P5 (GPCMV/full) but not CA-P5 (GPCMV/del) (Fig. 4A), indicating the specificity of the antibody. Both anti-GP131 (Fig. 4B) and anti-FLAG tag (data not shown) antibodies detected diffuse signals in cytoplasm of the 293T and GPL cells that were fixed with acetone 48 h after transfection of

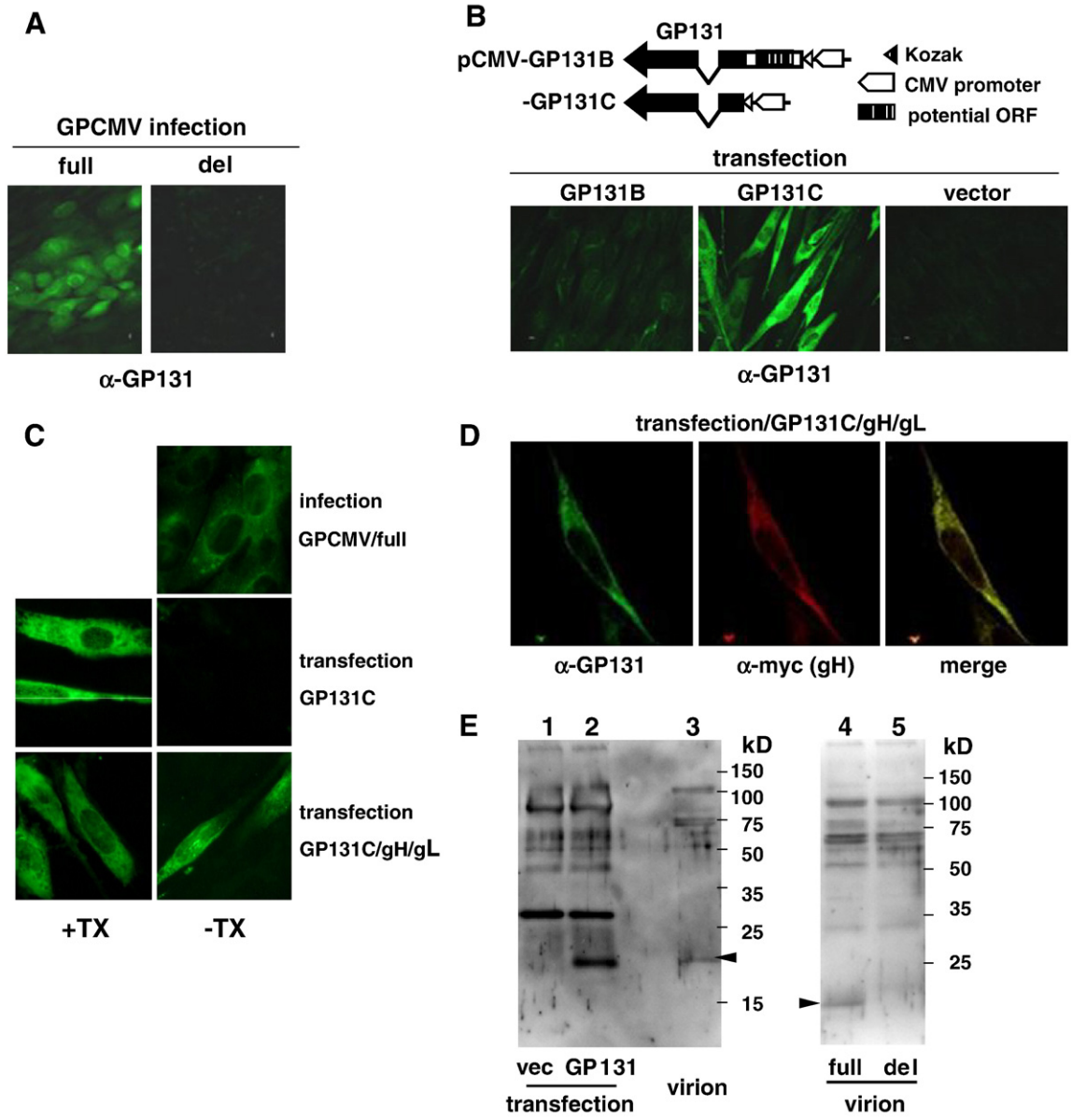

Fig. 4. Expression of pGP131. (A) GPL cells were infected with GPCMV CD-P5 (full) or CA-P5 (del) stock, and cultured for 5 days. The cells were fixed with acetone, incubated with anti-GP131 antibody followed by FITC-conjugated anti-rabbit IgG antibody. (B) GPL cells were transfected with one of the plasmids, pCMV-GP131B, -GP131C, and -Tag4A (vector), and cultured for 48 h. Structures of the plasmids are shown schematically. The cells were reacted as described for panel A. (C) GPL cells were infected with GPCMV CD-P5 (full) and cultured for 5 days. Also GPL cells were transfected with pCMV-GP131C, or with a combination of pCMV-GP131C, -gH/Myc, and -gL/His, and cultured for 48 h. The infected or transfected cells were fixed with paraformaldehyde, treated with or without Triton-X100 (TX) for permeabilization, and then reacted with antibodies. (D) Confocal microscopic images of the GPL cells that were cotransfected with pCMV-GP131C, -gH/Myc, and -gL/His, and fixed with paraformaldehyde followed by Triton-X100 treatment. Anti-GP131 and anti-myc antibodies were reacted with FITC- (green) and TRITC- (orange) conjugated secondary antibodies, respectively. (E) Detection of pGP131 in virions. Extracts of GPL cells transfected with pCMV-Tag4A (vec: lane 1) or with pCMV-GP131C (GP131: lane 2) were immunoprecipitated with anti-GP131 antibody. The precipitated samples and partially-purified virion preparations of GPCMV/full (lanes 3 and 4) and GPCMV/del (lane 5) were run on 12% SDS-PAGE and analyzed by immunoblotting with anti-GP131 antibody. The number of viral particles run in each lane was 1×10^8 based on genome copy number. Arrowheads indicate the pGP131 band.

pCMV-GP131C, which encodes pGP131 with a FLAG tag. On the other hand, in the cells transfected with pCMV-GP131B plasmid, signals were almost undetectable. A potential 127 a.a. ORF, which can be identified just 14 bp from the start site of the same transcript may be involved in the decrease of pGP131 level.

Cell surface localization of pGP131 in the presence of gH/gL

pGP131 was detected on the surface of GPCMV-infected cells after paraformaldehyde fixation without permeabilization (Fig. 4C). In contrast, in cells transfected with pCMV-GP131C, pGP131 was only detectable after treatment of the paraformaldehyde-fixed cells with Triton-X100. Importantly, cotransfection of gH- and gL-expressing plasmids with pCMV-GP131C enabled cell surface expression of pGP131, suggesting that gH/gL is required for cell surface trafficking of pGP131.

Co-localization of pGP131 with gH (Fig. 4D) and with gL (data not shown) was demonstrated by analysis of the cells cotransfected with pCMV-GP131C, -gH/Myc, and -gL/His in confocal microscopy. These data suggest that pGP131 forms a complex with gH/gL.

pGP131 is present in virions

pGP131 in GPL cells was immunoprecipitated with anti-GP131 antibody, and then detected as a 20-kD band in immunoblotting with the same antibody (Fig. 4E, lane 2). Probably due to the small amount of the protein, enrichment of the protein by immunoprecipitation was needed. The same size band was detected with a partially-purified GPCMV/full virion sample (Fig. 4E, lanes 3 and 4) but not with GPCMV/del one (lane 5), indicating that pGP131 is a virion component. The viral antigen recognized by the monoclonal antibody g-1 (Katano et al., 2007), which is localized in nuclei of infected cells but not in virion, was undetectable in the virion preparations used in this study (data not shown).

Discussion

In this study, we found the following: i) the 1.6 kb locus essential for efficient in vivo dissemination of GPCMV encodes homologs of HCMV UL128 and UL130, i.e. *GP129* and *GP131*, respectively, ii) these genes were expressed with late gene kinetics, iii) expression of pGP131 on cell surface required co-expression of gH and gL, iv) pGP131 colocalized with gH and gL, and v) pGP131 is a virion component. Therefore, it is likely that GPCMV pGP131 has function similar to pUL130.

From an evolutionary perspective, the GPCMV genome has chimeric characteristics between rodent and primate CMVs. GPCMV encodes a homolog of MCMV and RCMV ie2 genes (*M128* and *R128*), which are not found in primate CMVs. In contrast, GPCMV encodes homologs of HCMV UL128 and UL130, which are identified in most primate CMVs, including chimpanzee, rhesus, and simian CMVs (Akter et al., 2003; Rivailler et al., 2006); in place of UL128 and UL130, rodent CMVs encode CC-chemokine-like products, which are essential for efficient virus growth in vivo (Saederup et al., 1999; MacDonald et al., 1999; Voigt et al., 2005; Manning et al., 1992). Curiously, GPCMV apparently does not encode for a homolog of HCMV UL131A that is considered indispensable for infection of the epithelial/endothelial/leukocyte cell types (Adler et al., 2006; Hahn et al., 2004; Ryckman et al., 2008b; Wang and Shenk, 2005a). Identification and characterization of CMVs from animals that are evolutionarily intermediate from guinea pigs to primates, as well as from rats to guinea pigs, may contribute to better understanding of how UL128–131A gene homologs were acquired or created.

Several studies have demonstrated that HCMV pUL128, pUL130 and pUL131A are individually indispensable for infection of endothelial and epithelial cells (Adler et al., 2006; Wang and Shenk, 2005a; Wang et al., 2007; Ryckman et al., 2006). Inefficient growth of RhCMV 68-1, an RhCMV strain lacking *UL128* and a part of *UL130*, in epithelial cells was overcome by the repair of these genes, and the repaired RhCMV could grow even in human endothelial and epithelial cells (Lilja and Shenk, 2008). In our previous study, we demonstrated that the 1.6 kb locus containing the *GP129* and *GP131* genes was indispensable for growth in vivo but not in fibroblast cells in vitro, and discussed that our study was limited by an absence of experimental evidence demonstrating expression of GP129 and GP131 was directly associated with an altered cell tropism. In the case of GPCMV, the lack of easily available guinea pig endothelial and epithelial cells as well as of commercial antibodies against particular cell types of guinea pigs hinders evaluation of GP129 and GP131 for involvement in cell tropisms. Unfortunately, there is not yet any BAC system for examination of GPCMV growth in animals, since the GPCMV-BAC clone initially used for biological analysis by others lacks the 1.6 kb locus (Schleiss et al., 2008). The recently developed excisable GPCMV-BAC clone pN13R10 (Cui et al., 2008a) has a 4-bp deletion in GP129 exon 3 at position 8908 (data not shown), and the growth of GPCMV recovered from the BAC clone in animals has not been characterized. Therefore, we still lack a system for in vivo genetic evaluation of the functions of pGP129 and pGP131.

HCMV pUL128–pUL131A form a complex with gH and gL, and co-expression of pUL128–pUL131A with gH/gL is required for efficient transport of gH/gL/pUL128–pUL131A complex from the ER to the Golgi apparatus and then for extracellular secretion of the soluble form of the complex (Ryckman et al., 2008b). It was proposed that the gH/gL/pUL128–pUL131A complex binds to a cell-specific receptor (Ryckman et al., 2008a) and that at least pUL128 is directly involved in the receptor binding (Patrone et al., 2007). Biological similarity of GPCMV pGP131 with HCMV pUL130 can be assumed based on our findings of: i) sequence similarity between GP131 and UL130, ii) incorporation of pGP131 into virions, iii) cell surface expression of pGP131 only in the presence of gH and gL, and iv) colocalization of pGP131 with gH and with gL. However, since the amount of pGP131 expressed in vitro was insufficient for biochemical analysis, further study will be required to learn whether pGP131 interacts directly with gH/gL. Recent studies demonstrated that antibodies against pUL128, pUL130 and pUL131A neutralized virus infection of endothelial and epithelial cells and inhibited virus transfer from HCMV-infected cells to leukocytes (Gerna et al., 2008). Human immune sera have higher neutralizing activities against epithelial cell entry compared to fibroblast entry, and epithelial entry-specific neutralizing activities induced by the Towne and gB vaccines were lower than those observed following natural infection (Cui et al., 2008b). These observations suggest that subunit vaccines based on pUL128, pUL130 and pUL131A might be effective and could cooperate with the gB subunit vaccine. For that purpose, analyses in guinea pigs of immunologic reactions to GPCMV pGP129 and pGP131 may provide useful insights, since previous studies by us and others (Katano et al., 2007; Schleiss, 2006) demonstrated that the virus with the 1.6 kb region, or the salivary grand-passaged virus, crossed the placenta and infected fetus.

Materials and methods

Cells, viruses, and animals

Guinea pig lung fibroblasts (GPL, ATCC CCL-158) were cultured in F-12 medium supplemented with 10% fetal bovine serum (FBS), and after infection with GPCMV, in F-12 medium supplemented with 2% FBS. GPL cells were infected with GPCMV strain 22122 purchased from ATCC (VR-682). The infected cells (TC-P1) were propagated by co-culturing with uninfected GPL cells at a ratio of 1:5–1:10 four times to prepare a large stock of cell-free virus (TC-P5). Preparation of stocks of ten independent virus clones (CA-P5 to CJ-P5) was described

previously (Nozawa et al., 2008). From them, CD-P5 and CA-P5 were used here as GPCMV/full and GPCMV/del, respectively. GPCMV stocks were also prepared from salivary glands (SG) of a guinea pig (Hartley strain) infected with the TC-P5 stock. SG were minced, sonicated briefly, and then centrifuged to remove debris. These supernatants (SG-P0) were used for infection of GPL cells, and viral stocks were prepared after propagation of the cell-free virus 5 times in GPL cells (SG-P5). Partially-purified virions were prepared as follows. After removal of cell debris by centrifugation, supernatants of GPCMV-infected cells were loaded on a sucrose gradient (30% and 50% sucrose in PBS) and centrifuged at 82,000 $\times g$ for 2 h. The particles between the sucrose layers were collected and then precipitated by centrifugation.

Five-week old female guinea pigs (Hartley, Japan SLC, Inc.) were inoculated intra-peritonealy (i.p.) with 10^6 PFU of GPCMV. Blood specimens drawn directly from heart, and organ specimens, including liver, spleen, kidney, lung, and salivary gland, were harvested at indicated days after inoculation. All animal procedures were approved by the Animal Care and Use Committee of the National Institute of Infectious Diseases (NIID), and were conducted according to 'the Guidelines for Animal Experiments Performed at the NIID'.

Sequencing

Two 6 to7 kb fragments spanning the 13 kb region of GPCMV were amplified by PCR using KOD-FX polymerase (Toyobo, Japan) with primer sets S1 and S2 (Supplementary table 1), and purified by using a commercial kit (QIAEXII, Qiagen). A commercial kit (BigDye Terminator Cycle Sequencing Kit ver. 3.3, PE Applied Biosystems) was used for sequencing of these fragments, and the reactions were analyzed in the ABI PRISM 7500 sequence detection system (PE Applied Biosystems). Data were assembled and analyzed by using the programs ATGC and GENETYX (Genetyx Inc., Tokyo, Japan). The 13 kb sequence obtained from GPCMV DNA prepared from the salivary gland of an infected animal was deposited to DDBJ (accession no. AB492278).

RACE

GPL cells were infected with GPCMV at a multiplicity of infection (MOI) of 5, and cultured for 3 days. Total RNA samples were prepared by using RNeasy Plus Mini kit (Qiagen). The RACE reactions were done by using a commercial kit (SMART RACE cDNA Amplification Kit, Clontech) as described in the manufacturer's instructions. Sequences of the RACE products were determined as described above.

Northern blotting

GPL cells were infected with GPCMV at an MOI of 5, cultured in the absence or presence of 0.3 mg/ml PAA, and harvested at 6, 10, 24, 48, and 72 h after infection. 2 μg of total RNA prepared as described above was run on 1.0 % agarose gels containing formaldehyde and blotted onto Hybond H+ membranes (GE Healthcare). DNA fragments prepared by PCR using primer sets S3, S4 and S5 (Supplementary table 1) were used as probes for hybridization. The hybridized signals were detected by using a commercial kit (ECL Direct Labeling and Detection System, GE Healthcare).

Quantitative RT-PCR

Quantitative RT-PCR assays were carried out as described previously (Nozawa et al., 2008). Primer and probe sets S6-S10 were used for detection of *GP89* (terminase gene), GP131, GP129, and β-actin transcripts (Supplementary table 1).

Construction of plasmids

A fragment was amplified from overlapping 5′ and 3′ RACE products for the *GP131* gene by PCR using Pfu polymerase (Promega) with a primer set S11, and cloned between XhoI and NotI sites of pCMV-Tag4 (Stratagene), resulting in pCMV-GP131A. Fragments amplified from pCMV-GP131A with primer sets S12 and S13, respectively, were cloned into pCMV-Tag4, resulting in pCMV-GP131B and -GP131C (Fig. 4B). Fragments containing gH and gL ORFs were amplified from plasmids of a GPCMV genome library using KOD-FX polymerase with primer sets S14 and S15, respectively. The gH fragment was cloned into pA3M, which adds three myc epitope-tags at the carboxyl-terminus (Aster et al., 1997), resulting in pCMV-gH/Myc, and the gL fragment into pcDNA6/V5-His (Invitrogen), which adds a His tag at the carboxyl-terminus, resulting in pCMV-gL/His.

Preparation of antibody against pGP131

A DNA fragment containing a part of GP131 ORF (a.a. position 13 to 192) was amplified by PCR with a primer set S16 (Supplementary table 1) and cloned into pGEX-6P-1 vector (GE Healthcare). The GST-GP131 fusion protein was expressed in BL21 cells (Invitrogen) upon addition of IPTG. Insoluble inclusion bodies, containing the GST-GP131 fusion protein, were prepared from the cells and solubilized in 8 M urea. The samples were diluted eight fold with PBS containing 0.5% Triton-X100 and purified by glutathione-sepharose column (GE Healthcare). Finally, a rabbit was immunized with the GST-GP131 fusion protein (Japan Biotest Corporation).

Immunofluorescence assay (IFA)

Transfection of cells was performed by using a commercial reagent (Fugene 6, Roche). GPCMV-infected and transfected cells were fixed with acetone for 5 min or with 4% paraformaldehyde for 15 min followed by treatment with 0.1 % Triton X-100 for 10 min. Anti-GP131 rabbit antibody and anti-myc monoclonal antibody 9E10 (Santa Cruz) were used as primary antibodies, and FITC-conjugated anti-rabbit IgG and TRITC-conjugated anti-mouse IgG antibodies were used as secondary antibodies. Confocal images were captured with a LSM5 PASCAL digital confocal microscope (Zeiss), and analyzed by using its LSM Image Browser.

Immunoprecipitation and immunoblotting

Transfected or infected cells were incubated in a Lysis buffer containing 50 mM Tris–HCl (pH 8.0), 150 mM NaCl, 1% NP-40, and 1 mM phenyl-methylsulfonyl fluoride (PMSF) for 20 min. After centrifugation at 9000 $\times g$ for 15 min, supernatants were recovered as cell extracts. The extracts were pre-cleared with protein G-agarose (GE Healthcare) for 1 h and then immunoprecipitated using anti-GP131 polyclonal rabbit antibody along with protein G-agarose for 1 h. The resin was washed in the Lysis buffer 4 times. Proteins bound to the resin were eluted by boiling in 4% SDS and 10% 2-mercaptoethanol, separated in a 12% SDS-polyacrylamide gel, and then transferred to a Hybond-P membrane (GE healthcare) for immunoblotting. Immunoblot reactions were done as described previously (Koyano et al., 2003).

Acknowledgments

We thank Mike McVoy for GPCMV-BAC clone pN13R10 DNA, Phil Pellett for his intellectual input, Yumiko Yamamoto, Yuhki Inami, and Yuko Sato for their technical assistance. This work was supported by grants for Research Promotion of Emerging and Re-emerging Infectious Diseases from the Ministry of Health, Labor and Welfare, Japan (H18-Shinko-13 and H21-Shinko-Ippan-009), to NI.

Appendix A. Supplementary data

Supplementary data associated with this article can be found, in the online version, at doi:10.1016/j.virol.2009.05.034.

References

Adler, B., Scrivano, L., Ruzcics, Z., Rupp, B., Sinzger, C., Koszinowski, U., 2006. Role of human cytomegalovirus UL131A in cell type-specific virus entry and release. J. Gen. Virol. 87, 2451–2460.

Akter, P., Cunningham, C., McSharry, B.P., Dolan, A., Addison, C., Dargan, D.J., Hassan-Walker, A.F., Emery, V.C., Griffiths, P.D., Wilkinson, G.W., Davison, A.J., 2003. Two novel spliced genes in human cytomegalovirus. J. Gen. Virol. 84, 1117–1122.

Aster, J.C., Robertson, E.S., Hasserjian, R.P., Turner, J.R., Kieff, E., Sklar, J., 1997. Oncogenic forms of NOTCH1 lacking either the primary binding site for RBP-Jkappa or nuclear localization sequences retain the ability to associate with RBP-Jkappa and activate transcription. J. Biol. Chem. 272, 11336–11343.

Cha, T.A., Tom, E., Kemble, G.W., Duke, G.M., Mocarski, E.S., Spaete, R.R., 1996. Human cytomegalovirus clinical isolates carry at least 19 genes not found in laboratory strains. J. Virol. 70, 78–83.

Cui, X., McGregor, A., Schleiss, M.R., McVoy, M.A., 2008a. Cloning the complete guinea pig cytomegalovirus genome as an infectious bacterial artificial chromosome with excisable origin of replication. J. Virol. Methods 149, 231–239.

Cui, X., Meza, B.P., Adler, S.P., McVoy, M.A., 2008b. Cytomegalovirus vaccines fail to induce epithelial entry neutralizing antibodies comparable to natural infection. Vaccine 26, 5760–5766.

Dolan, A., Cunningham, C., Hector, R.D., Hassan-Walker, A.F., Lee, L., Addison, C., Dargan, D.J., McGeoch, D.J., Gatherer, D., Emery, C., Griffiths, P.D., Sinzger, C., McSharry, B.P., Wilkinson, G.W., Davison, A.J., 2004. Genetic content of wild-type human cytomegalovirus. J. Gen. Virol. 85, 1301–1312.

Gerna, G., Baldanti, F., Revello, M.G., 2004. Pathogenesis of human cytomegalovirus infection and cellular targets. Hum. Immunol. 65, 381–386.

Gerna, G., Sarasini, A., Patrone, M., Percivalle, E., Fiorina, L., Campanini, G., Gallina, A., Baldanti, F., Revello, M.G., 2008. Human cytomegalovirus serum neutralizing antibodies block virus infection of endothelial/epithelial cells, but not fibroblasts, early during primary infection. J. Gen. Virol. 89, 853–865.

Grundy, J.E., Lawson, K.M., MacCormac, L.P., Fletcher, J.M., Yong, K.L., 1998. Cytomegalovirus-infected endothelial cells recruit neutrophils by the secretion of C-X-C chemokines and transmit virus by direct neutrophil–endothelial cell contact and during neutrophil transendothelial migration. J. Infect. Dis. 177, 1465–1474.

Hahn, G., Revello, M.G., Patrone, M., Percivalle, E., Campanini, G., Sarasini, A., Wagner, M., Gallina, A., Milanesi, G., Koszinowski, U., Baldanti, F., Gerna, G., 2004. Human cytomegalovirus UL131–128 genes are indispensable for virus growth in endothelial cells and virus transfer to leukocytes. J. Virol. 78, 10023–10033.

Hopp, T.P., Woods, K.R., 1981. Prediction of protein antigenic determinants from amino acid sequences. Proc. Natl. Acad. Sci. U. S. A. 78, 3824–3828.

Katano, H., Sato, Y., Tsutsui, Y., Sata, T., Maeda, A., Nozawa, N., Inoue, N., Nomura, Y., Kurata, T., 2007. Pathogenesis of cytomegalovirus-associated labyrinthitis in a guinea pig model. Microbes. Infect. 9, 183–191.

Kern, E.R., 2006. Pivotal role of animal models in the development of new therapies for cytomegalovirus infections. Antiviral. Res. 71, 164–171.

Koyano, S., Inoue, N., Nagamori, T., Yan, H., Asanuma, H., Yagyu, K., Osaki, M., Seiwa, C., Fujieda, K., 2009. Dried umbilical cords in the retrospective diagnosis of congenital cytomegalovirus infection as a cause of developmental delays. Clin. Infec. Dis. 48, e93–e95.

Koyano, S., Mar, E.C., Stamey, F.R., Inoue, N., 2003. Glycoproteins M and N of human herpesvirus 8 form a complex and inhibit cell fusion. J. Gen. Virol. 84, 1485–1491.

Lilja, A.E., Shenk, T., 2008. Efficient replication of rhesus cytomegalovirus variants in multiple rhesus and human cell types. Proc. Natl. Acad. Sci. U. S. A. 105, 19950–19955.

MacDonald, M.R., Burney, M.W., Resnick, S.B., Virgin IV, H.W., 1999. Spliced mRNA encoding the murine cytomegalovirus chemokine homolog predicts a beta chemokine of novel structure. J. Virol. 73, 3682–3691.

Manning, W.C., Stoddart, C.A., Lagenaur, L.A., Abenes, G.B., Mocarski, E.S., 1992. Cytomegalovirus determinant of replication in salivary glands. J. Virol. 66, 3794–3802.

Murphy, E., Yu, D., Grimwood, J., Schmutz, J., Dickson, M., Jarvis, M.A., Hahn, G., Nelson, J. A., Myers, R.M., Shenk, T.E., 2003. Coding potential of laboratory and clinical strains of human cytomegalovirus. Proc. Natl. Acad. Sci. U. S. A. 100, 14976–14981.

Nozawa, N., Yamamoto, Y., Fukui, Y., Katano, H., Tsutsui, Y., Sato, Y., Yamada, S., Inami, Y., Nakamura, K., Yokoi, M., Kurane, I., Inoue, N., 2008. Identification of a 1.6 kb genome locus of guinea pig cytomegalovirus required for efficient viral growth in animals but not in cell culture. Virology 379, 45–54.

Ogawa, H., Suzutani, T., Baba, Y., Koyano, S., Nozawa, N., Ishibashi, K., Fujieda, K., Inoue, N., Omori, K., 2007. Etiology of severe sensorineural hearing loss in children: independent impact of congenital cytomegalovirus infection and GJB2 mutations. J. Infect. Dis. 195, 782–788.

Pass, R.F., 2001. Cytomegalovirus. In: Knipe, D.M., Howley, P.M. (Eds.), Fields Virology, 2. Lippincott Williams & Wilkins, Philadelphia, PA, pp. 2675–2705.

Patrone, M., Secchi, M., Bonaparte, E., Milanesi, G., Gallina, A., 2007. Cytomegalovirus UL131-128 products promote gB conformational transition and gB–gH interaction during entry into endothelial cells. J. Virol. 81, 11479–11488.

Rivailler, P., Kaur, A., Johnson, R.P., Wang, F., 2006. Genomic sequence of rhesus cytomegalovirus 180.92: insights into the coding potential of rhesus cytomegalovirus. J. Virol. 80, 4179–4182.

Ryckman, B.J., Chase, M.C., Johnson, D.C., 2008a. HCMV gH/gL/UL128–131 interferes with virus entry into epithelial cells: evidence for cell type-specific receptors. Proc. Natl. Acad. Sci. U. S. A. 105, 14118–14123.

Ryckman, B.J., Jarvis, M.A., Drummond, D.D., Nelson, J.A., Johnson, D.C., 2006. Human cytomegalovirus entry into epithelial and endothelial cells depends on genes UL128 to UL150 and occurs by endocytosis and low-pH fusion. J. Virol. 80, 710–722.

Ryckman, B.J., Rainish, B.L., Chase, M.C., Borton, J.A., Nelson, J.A., Jarvis, M.A., Johnson, D.C., 2008b. Characterization of the human cytomegalovirus gH/gL/UL128–131 complex that mediates entry into epithelial and endothelial cells. J. Virol. 82, 60–70.

Saederup, N., Lin, Y.C., Dairaghi, D.J., Schall, T.J., Mocarski, E.S., 1999. Cytomegalovirus-encoded beta chemokine promotes monocyte-associated viremia in the host. Proc. Natl. Acad. Sci. U. S. A. 96, 10881–10886.

Schleiss, M.R., 2006. Nonprimate models of congenital cytomegalovirus (CMV) infection: gaining insight into pathogenesis and prevention of disease in newborns. ILAR J. 47, 65–72.

Schleiss, M.R., McGregor, A., Choi, K.Y., Date, S.V., Cui, X., McVoy, M.A., 2008. Analysis of the nucleotide sequence of the guinea pig cytomegalovirus (GPCMV) genome. Virol. J. 5, 139.

Schuessler, A., Sampaio, K.L., Sinzger, C., 2008. Charge cluster-to-alanine scanning of UL128 for fine tuning of the endothelial cell tropism of human cytomegalovirus. J. Virol. 82, 11239–11246.

Voigt, S., Sandford, G.R., Hayward, G.S., Burns, W.H., 2005. The English strain of rat cytomegalovirus (CMV) contains a novel captured CD200 (vOX2) gene and a spliced CC chemokine upstream from the major immediate-early region: further evidence for a separate evolutionary lineage from that of rat CMV Maastricht. J. Gen. Virol. 86, 263–274.

Wang, D., Shenk, T., 2005a. Human cytomegalovirus UL131 open reading frame is required for epithelial cell tropism. J. Virol. 79, 10330–10338.

Wang, D., Shenk, T., 2005b. Human cytomegalovirus virion protein complex required for epithelial and endothelial cell tropism. Proc. Natl. Acad. Sci. U. S. A. 102, 18153–18158.

Wang, D., Yu, Q.C., Schroer, J., Murphy, E., Shenk, T., 2007. Human cytomegalovirus uses two distinct pathways to enter retinal pigmented epithelial cells. Proc. Natl. Acad. Sci. U. S. A. 104, 20037–20042.